Article

A Ratiometric and Colorimetric Hemicyanine Fluorescent Probe for Detection of SO$_2$ Derivatives and Its Applications in Bioimaging

Yan-Hong Qin [1,†], Xiao-Yi Jiang [1,†], Yuan-Fang Que [1], Jing-Yi Gu [1], Tong Wu [1], Ayinazhaer Aihemaiti [1], Ke-Xin Shi [1], Wen-Yu Kang [1], Bi-Ying Hu [1], Jin-Shuai Lan [1,2,*], Yue Ding [1,2] and Tong Zhang [1,2,*]

[1] School of Pharmacy, Shanghai University of Traditional Chinese Medicine, Shanghai 201203, China; 15002120171@163.com (Y.-H.Q.); Joy213_8327@163.com (X.-Y.J.); qyf2016here@163.com (Y.-F.Q.); q771577634@163.com (J.-Y.G.); 13501919930@163.com (T.W.); Aynazar0601@163.com (A.A.); Skx_gulala93@163.com (K.-X.S.); kangwenyu274@163.com (W.-Y.K.); hby4477jy@163.com (B.-Y.H.); dingyue1640@shutcm.edu.cn (Y.D.)

[2] Experiment Center of Teaching & Learning, Shanghai University of Traditional Chinese Medicine, Shanghai 201203, China

* Correspondence: lanjinshuai_shut@126.com (J.-S.L.); zhangtongshutcm@hotmail.com (T.Z.); Tel.: +86-021-5132-2318 (J.-S.L.)

† These authors contributed equally to this work.

Abstract: Based upon the intramolecular charge transfer (ICT) mechanism, a novel ratiometric fluorescent probe **EB** was developed to detect SO_3^{2-}/HSO_3^-. The probe displayed both colorimetric and ratiometric responses toward SO_3^{2-}/HSO_3^-. It displayed a quick response (within 60 s), good selectivity and high sensitivity (a detection limit of 28 nM) towards SO_3^{2-}/HSO_3^-. The SO_3^{2-}/HSO_3^- sensing mechanism was confirmed as the Michael addition reaction by ESI-MS. Moreover, the probe could be applied to measure the level of sulfite in real samples, like sugar and chrysanthemum, and it could also be used to detect SO_3^{2-}/HSO_3^- in HepG2 cells through confocal fluorescence microscopy, which proved its practical application in clinical diagnosis.

Keywords: SO$_2$ derivatives; ratiometric fluorescent probe; bioimaging

1. Introduction

Sulfur dioxide (SO$_2$), as one of the most serious atmospheric pollutants, can enter the living organisms through the respiratory system and then can be turned into sulfite (SO_3^{2-})/bisulfate (HSO_3) in aqueous [1–3]. Although these endogenous derivatives in organisms have some functions for relaxing the vascular smooth muscle and resisting oxidation [4–6], SO$_2$ could cause diseases in the respiratory system, the nervous system and the cardiovascular system, such as strokes, asthmatic attacks, migraine headaches, allergic reactions and ischemic heart diseases [7–10]. Considering the relationship between SO$_2$ and the above-mentioned potential health problems, many countries have enforced strict regulations of the concentrations of SO_3^{2-}/HSO_3^- in food, beverages and medicine. Therefore, effective analytical methods were developed to test the SO_3^{2-}/HSO_3^- concentrations in vitro and in vivo, which is essential for the accurate determination of the biological activity of SO$_2$ derivatives [11,12].

Compared with traditional detection methods like titration [13], electrochemistry [14,15] and capillary electrophoresis [16,17], fluorescent probes have strengths in operation, sensitivity and selectivity, and can be applied in real-time bioimaging in vivo. Fluorescent probes based on the

(*E*)-1,1,3-trimethyl-2-styryl-1*H*-benzo[e]indol-3-ium platform are popular because of their strong fluorescence, good water solubility and relatively large Stokes shift. For example, based on the skeleton (*E*)-1,1,3-trimethyl-2-styryl-1*H*-benzo[e]indol-3-ium with acetyl substitution, a probe reported by Zhou et al. can usefully test carboxylesterase [18]. Nowadays, there are some fluorescent probes based on different reaction mechanisms to detect SO_3^{2-}/HSO_3^-, such as 1,4-Michael addition [19–22], nucleophilic 1,2-addition [11,23] and deprotection of levulinate [24]. However, most fluorescent probes were based on limitedly single fluorescence changes, which will be influenced due to fluctuations in the system and the probe's concentration. For example, a probe reported by Yu et al. can usefully test SO_3^{2-}/HSO_3^-, but a single fluorescence change was used, which limited its use [25]. While the ratiometric fluorescent probes can gain more accurate results for its capacity to detect fluorescence emission/excitation intensities at two different wavelengths [26,27]. Therefore, compared with the single fluorescent probes, it is evitable for the ratiometric fluorescent probes to be influenced by the environmental changes [28]. Based on the ratiometric fluorescent probes, a probe with CF_3 substitution reported by Sun et al. can usefully test SO_3^{2-}/HSO_3^-, but the probe also reacted with CN^-, which was a low selectivity for its practical applications [19]. In order to develop new fluorescent probes for SO_3^{2-}/HSO_3^- detection [29], we paid more attention to developing a ratiometric probe that could satisfy the practical applications.

On account of the ideas above, we first developed a novel ratiometric fluorescent probe **EB** (*E*)-3-ethyl-2-(4-hydroxystyryl)-1,1-dimethyl-1*H*-benzo[e]indol-3-ium iodide for sensing SO_3^{2-}/HSO_3^- (Scheme 1), which is based on the nucleophilic reaction between SO_3^{2-}/HSO_3^- and the C=C bond. The 3-ethyl-1,1,2-trimethyl-1*H*-benzo[e]indol-3-ium iodide (the hemicyanine part) and 4-hydroxybenzaldehyde were used to synthesize the probe as the intramolecular charge transfer (ICT) donor and the acceptor respectively [30,31]. The hemicyanine was proved to be the effective fluorophores in designing fluorescent chemosensors, which had a blue fluorescence with high quantum efficiency and the chemical stability [20,32–34]. After the specific 1,4-addition reaction of SO_3^{2-}/HSO_3^- with the vinyl group of probe **EB** (Scheme 1), the structure of probe **EB** was destroyed by SO_2 derivatives. Therefore, because of the obvious emission between probe **EB** and the hemicyanine derivative, we could detect two well-resolved emission bands before and after addition of SO_3^{2-}/HSO_3^-. Thus, we could observe significant changes in the UV-Vis absorption spectra and fluorescence spectra and make the colorimetric and fluorogenic detection of SO_3^-/HSO_3^{2-} possible. Scheme 2 showed the synthesis route of probe **EB** and the structure of probe **EB** was confirmed by ^{1}H-NMR, ^{13}C-NMR and MS (Figures S1–S3). What's more, the probe showed excellent characteristics including the large hypsochromic shift, the ultrafast response time (within 60 s), high sensitivity (a detection limit of 28 nM), low cytotoxicity and excellent selectivity of SO_2 derivatives over other anions and biothiols. Additionally, it could effectively monitor SO_2 derivatives and successfully applied in real samples and living cells.
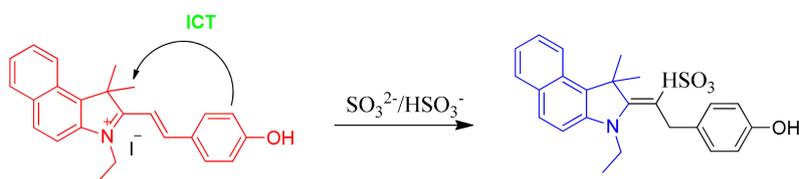
Scheme 1. Probe **EB** as a new ratiometric fluorescence probe for sensing of sulfite/bisulfite.
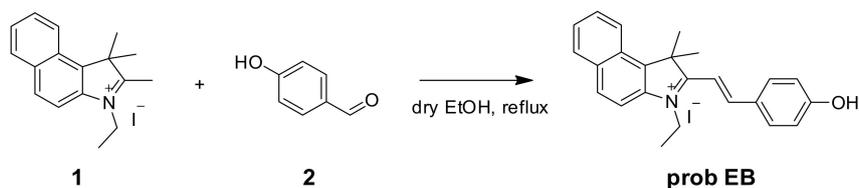
Scheme 2. Synthesis of probe **EB**.

2. Results and Discussion

2.1. UV-Vis and Fluorescence Spectra for Sulphite Detection

First, the UV-Vis absorption spectra of the probe were detected in PBS solution (pH = 7.4). As shown in Figure 1a, the UV-Vis absorption of probe **EB** showed an intense absorption peak at 510 nm, while the absorbance at 510 nm decreased dramatically after it had reacted with 500 μM SO_3^{2-}. At the same time, there was a significant color change: the obvious pink color of solution faded to colorless (Figures 1a and 1a inset), which suggested that a naked-eye colorimetric method could be used expediently to detect SO_3^{2-}/HSO_3^{-}. Next, due to the strong intramolecular charge transfer (ICT), probe **EB** (10 μM) showed a strong fluorescence peak at 570 nm (excitation at 485 nm), while with the increase of SO_3^{2-} (0–500 μM), the fluorescence emission band decreased dramatically at 570 nm (Figure 1b) and a new emission band simultaneously increased at 473 nm (excitation at 380 nm) (Figure 1c). The fluorescent quantum yield (Φ = 0.029) of probe **EB** at 570 nm and the fluorescent quantum yield (Φ = 0.537) of probe **EB** after reaction with 500 μM SO_3^{2-} at 473 nm has also been determined, with Rhodamine B as a reference. These changes were attributed to the transformation of the conjugated structure of the probe by reacting with SO_3^{2-}/HSO_3^{-}. What's more, there was a linear correlation between the fluorescence intensity ratios (I_{473}/I_{570}) and the concentration of SO_3^{2-} ranging from 0 to 60 μM (Figure 1d). According to the signal to noise ratio (S/N = 3), the limit of detection came out to be 28 nM, suggesting probe **EB** could be applied to detect traces of SO_3^{2-} under environmental or biological conditions.
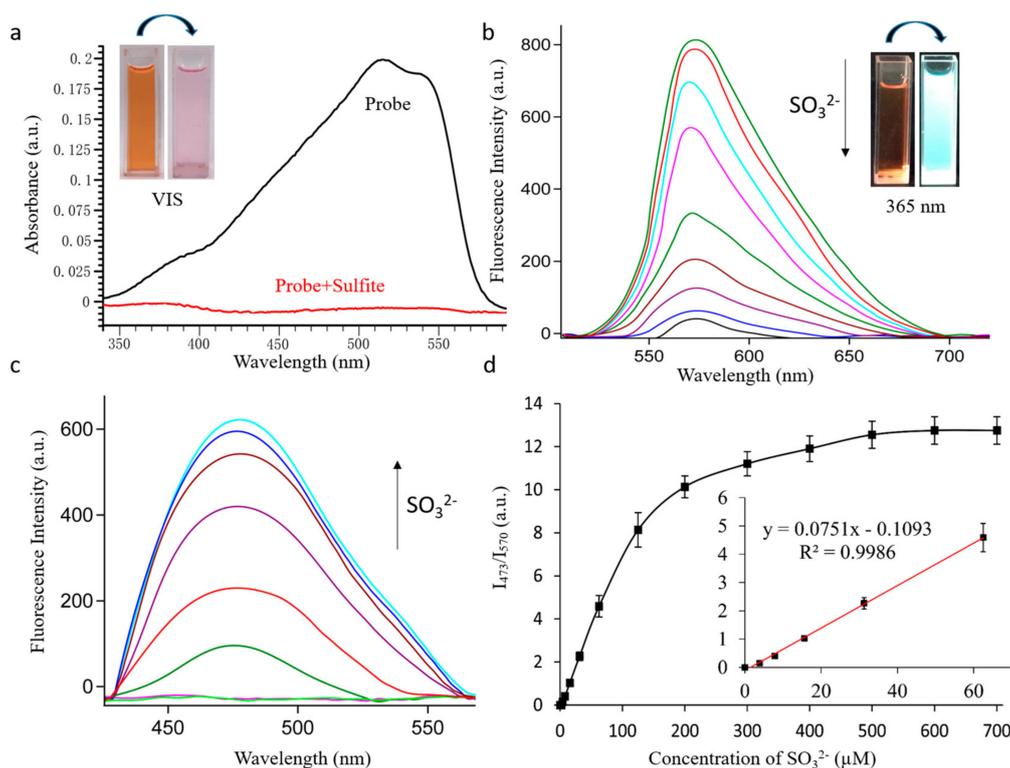
Figure 1. (**a**) UV-Vis absorption spectra changes and (**b**–**c**) fluorescence spectra changes of the probe **EB** (10 μM) in PBS solution (pH 7.4) with increasing amount of SO_3^{2-} (0–500 μM). For (**b**) λ_{ex} = 485 nm slits: 10.0/10.0 nm; for (**c**) λ_{ex} = 380 nm slits: 5.0/5.0 nm. (**d**) Linear correlation between the emission intensity ratio (I_{473}/I_{570}) and the concentration of SO_3^{2-}.

2.2. The Selective Response of Probe to Sulfite

The excellent selectivity of the probe played an essential role in practical application. In order to illustrate its anti-interference ability, we detected the fluorescence changes of probe **EB** (10 μM) with 500 μM other anions after 3 min, which aimed to prove no interference of the most common anions and biological thiols in the environment, including CO_3^{2-}, HCO_3^-, Ac^-, PO_4^{3-}, HPO_4^{2-}, $H_2PO_4^-$, Cl^-, Br^-, I^-, NO_2^-, S^{2-}, SO_4^{2-}, Hcy, Cys and GSH. As shown in Figure 2 (black), even 50 equivalents of the other species did not respond to the fluorescence ratio $I_{473}/_{570}$, but S^{2-} led to a slight increase of the fluorescence ratio $I_{473}/_{570}$, which may be influenced by the nucleophilicity of S^{2-}. Meanwhile, in Figure 2 (red), the competition experiments meant that other analytes did not influence on detecting SO_3^{2-} (500 μM). The results showed great selectivity of probe **EB** towards SO_3^{2-}, which indicated the excellent ability in the further application.
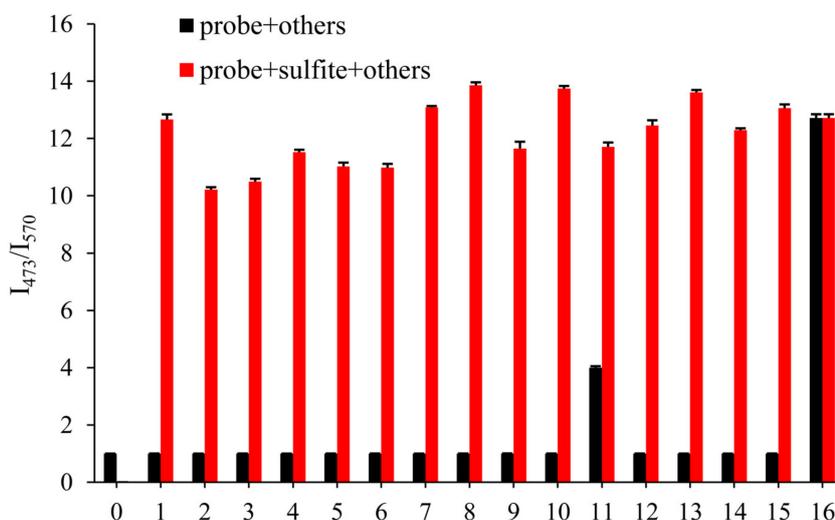
Figure 2. Fluorescence intensity of probe **EB** (10 μM) in PBS solution (pH 7.4) upon addition of various reactive sulphur and other anions (500 μM). 1. CO_3^{2-}, 2. HCO_3^-, 3. Ac^-, 4. PO_4^{3-}, 5. HPO_4^{2-}, 6. $H_2PO_4^-$, 7. Cl^-, 8. Br^-, 9. I^-, 10. NO_2^-, 11. S^{2-}, 12. SO_4^{2-}, 13. Hcy, 14. Cys and 15. GSH, 16. SO_3^{2-}. For λ_{ex} = 380 nm, λ_{em} = 473 slits: 5.0/5.0 nm; for λ_{ex} = 485 nm, λ_{em} = 570 nm slits: 10.0/10.0 nm.

2.3. Time-Dependence and pH-Dependence in the Detection Process of Sulfite

Time and pH are the pivotal factors, which could affect the application of the probe. Thus, with 500 μM SO_3^{2-}, we detected the fluorescent ratio ($I_{473}/_{570}$) changes of probe **EB** (10 μM) in different times (1–10 min) (Figure 3a). It showed that the fluorescent ratio ($I_{473}/_{570}$) of the probe tends to be stable in 1 min with the reaction of SO_3^{2-} (Figure 3a), implying the probe could act as a "fast response" fluorescent probe for SO_3^{2-} detection and may be used to timely sense SO_3^{2-} in living cells. Furthermore, the effect of pH on the fluorescent ratio ($I_{473}/_{570}$) of the probe to SO_3^{2-} was investigated ranging from pH 3 to 10. The fluorescent ratio ($I_{473}/_{570}$) of the probe was 0 without SO_3^{2-} when the pH ranged from 3 to 10 (Figure 3b), suggesting the probe kept stable within a broad pH range. By adding SO_3^{2-}, the fluorescent ratio ($I_{473}/_{570}$) of the probe increased rapidly to the peak at pH 8 and then dropped modestly, which indicated that in the normal physiological ranges (pH = 7.4), the probe could reliably detect SO_3^{2-}/HSO_3^-.
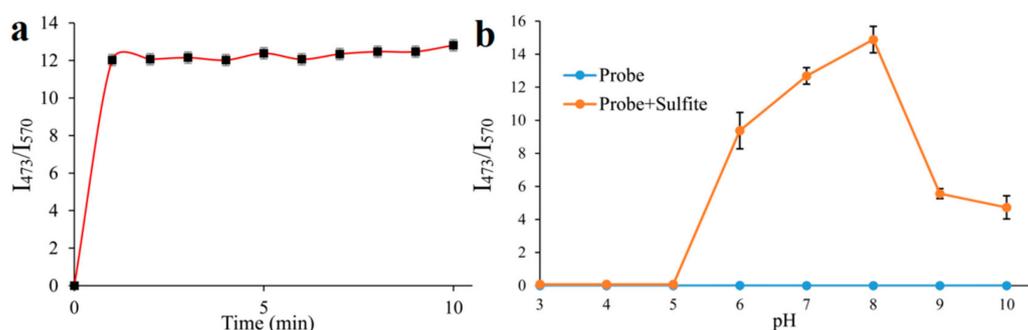
Figure 3. (**a**): Effect of time on the I_{473}/I_{570} fluorescence intensity ratio of probe **EB** (10 μM) in PBS solution (pH = 7.4) upon addition of 500 μM SO_3^{2-}; (**b**): Effect of pH on the I_{473}/I_{570} fluorescence intensity ratio of probe **EB** (10 μM) and probe **EB** upon addition of 500 μM SO_3^{2-}.

As described above, the probe displayed excellent analytical property comparing with some other fluorescent probes of recent reports for the detection of SO_3^{2-}/HSO_3^{-}. The comparison data are listed in Table S1, indicating that the probe is promising for practical analysis.

2.4. Reaction Mechanism

In order to monitor the reaction mechanism, ESI-MS was used to inspect the reaction between probe **EB** and SO_3^{2-}. In the ESI-MS spectrum (Figure 4), the main peak at m/z = 342.34 was assigned to probe **EB** (calculated: $[C_{20}H_{24}NO]^+$, 342.18). When Na_2SO_3 (10.0 equiv.) was added, the peak corresponds to probe-SO_3^{2-} appeared at m/z = 446.16 (calculated: $[C_{24}H_{24}NNaO_4S + H]^+$, 446.13). On the basis of the above experiment results, the reaction mechanism of probe **EB** with SO_3^{2-} was proposed and illustrated in Scheme 1, and it follows a 1,4-nucleophilic addition reaction of SO_3^{2-} to the vinyl group of probe **EB**.
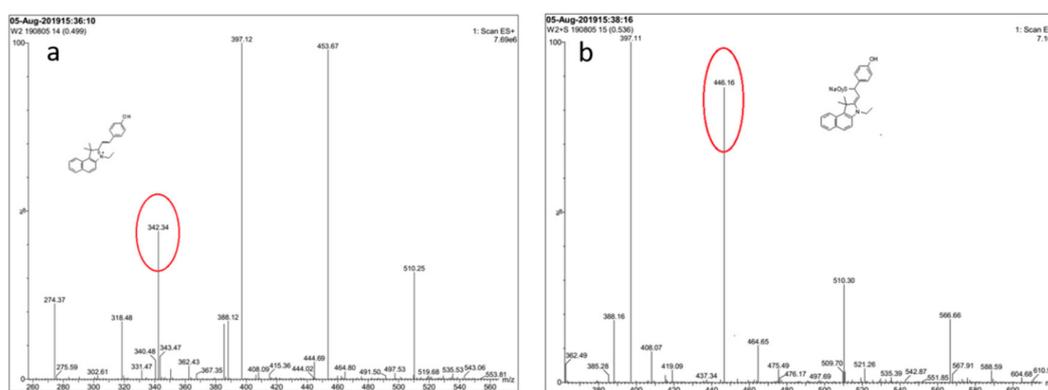
Figure 4. Mass spectrum of probe **EB** and the crude product of the probe with SO_3^{2-}. (**a**) Probe **EB** in MeOH. (**b**) Probe **EB** with Na_2SO_3 in MeOH: H_2O (1:1).

2.5. Sulfite Detection in Real Samples

In order to verify the practicability of the probe, we firstly investigated the sulfite levels in real samples by using probe **EB**, including tap water, river water, sugar water and chrysanthemum, which were dissolved and diluted in PBS solution (pH 7.4) into consistency for analysis. For comparison, a traditional titration method was used as validation. Two methods obtained almost consistent results (Table 1), which proved the practicability of probe **EB**. In addition, based on the above results, a standard addition method was used to detect sulfite in these real food samples. Adding an exact amount of SO_3^{2-} (25, 50 and 100 μM) to the diluted sample, the $I_{473/570}$ fluorescent ratio was measured. Excellent recovery ranged from 95.9% to 107.7% was observed in Table 1, suggesting the probe was practical and reliable for detecting sulfite in real samples.

Table 1. Determination of SO_3^{2-} in water samples using the probe **EB**.

Sample [a]	SO_3^{2-} Level Found (μM)	Added (μM)	Found (μM)	Recovery (%)
Tap water	0 [b]	25.0	24.99 ± 0.55	99.9
	0 [c]	50.0	48.87 ± 0.73	97.7
		100.0	95.92 ± 3.70	95.9
River water	1.8 ± 0.09 [b]	25.0	25.9 ± 0.96	96.6
	1.5 ± 0.18 [c]	50.0	52.4 ± 2.53	101.2
		100.0	102.3 ± 1.94	100.5
Sugar	0 [b]	25.0	25.1 ± 1.31	100.4
	0 [c]	50.0	52.9 ± 0.55	105.8
		100.0	104.8 ± 1.72	104.8
Chrysanthemum	16.8 ± 0.18 [b]	25.0	43.73 ± 2.38	107.7
	15.9 ± 0.25 [c]	50.0	69.2 ± 3.26	104.8
		100.0	115.9 ± 2.93	99.1

[a] In the detection solutions, the concentration of sugar was 5.0 g/100 mL (pH 7.4); the River water was diluted 3 times with PBS solution (pH 7.4); the chrysanthemum sample was extracted with PBS solution (pH = 7.4) as the test solution (0.5 g/100 mL).By means of the three measurements(n = 3), we obtained the standard derivations. [b] Analysis for SO_3^{2-} in water samples determined by the fluorescent probe. [c] Analysis for SO_3^{2-} in water samples determined by a traditional titration method.

2.6. Fluorescence Imaging in Living Cells

The application of the probe for cell bioimaging was studied based on the results above. Cytotoxicity experiment was firstly incubated in HepG2 cells using Cell Counting Kit-8 (CCK8), and as shown in Figure 5, the survival rate of HepG2 cells was about to reach 90 % after incubating with 100 μM probe **EB** for 24 h, which suggested that the probe has low cytotoxicity for application in living cells.
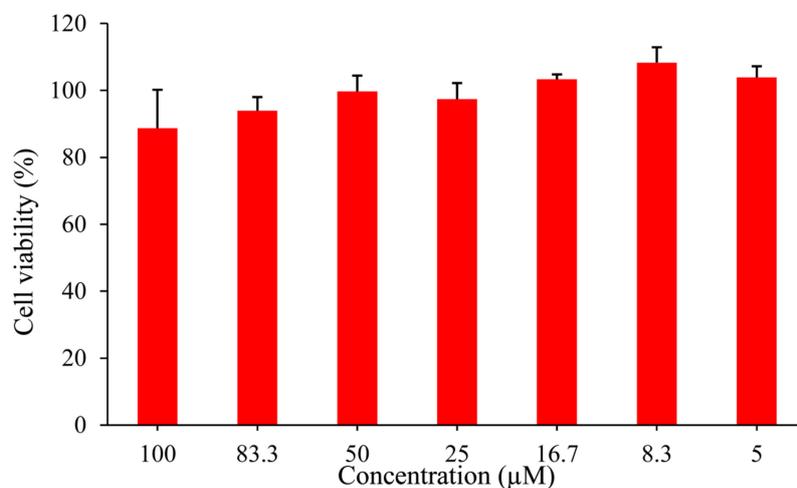
Figure 5. CCK8 assay of HepG2 cells incubated in the probe **EB** (0–100 μM) at 37 °C for 24 h.

To verify the biological applications of the probe, we tried to explore potentialities about detecting SO_3^{2-} in living cells. Firstly, we incubated the HepG2 with various concentrations of SO_3^{2-} (0, 10, 20, 50, 100, 200 μM) for 2 h. After that quantitative probe (10 μM) was added into all cell groups waiting for 2 h, and monitoring tests were operated by the confocal laser-scanning microscopy. HepG2 cells showed a clear red profile after the incubation with probe (10 μM) for 2 h (Figure 6a), which suggested that the probe **EB** could permeate into HepG2 cells. While HepG2 cells were incubated with different concentrations of SO_3^{2-} (0, 10, 20, 50, 100, 200 μM) for 2 h beforehand and then incubated with the probe **EB**. After 2 h, the fluorescence in the blue channel enhanced with the concentration of SO_3^{2-} raised, but the fluorescence under the red channel degraded (Figure 6a–f). Finally, the HepG2 cells

(Figure 6f) displayed strong blue fluorescence and weak red fluorescence. Therefore, the probe **EB** could be employed for the SO_3^{2-} fluorescence imaging in living cells.
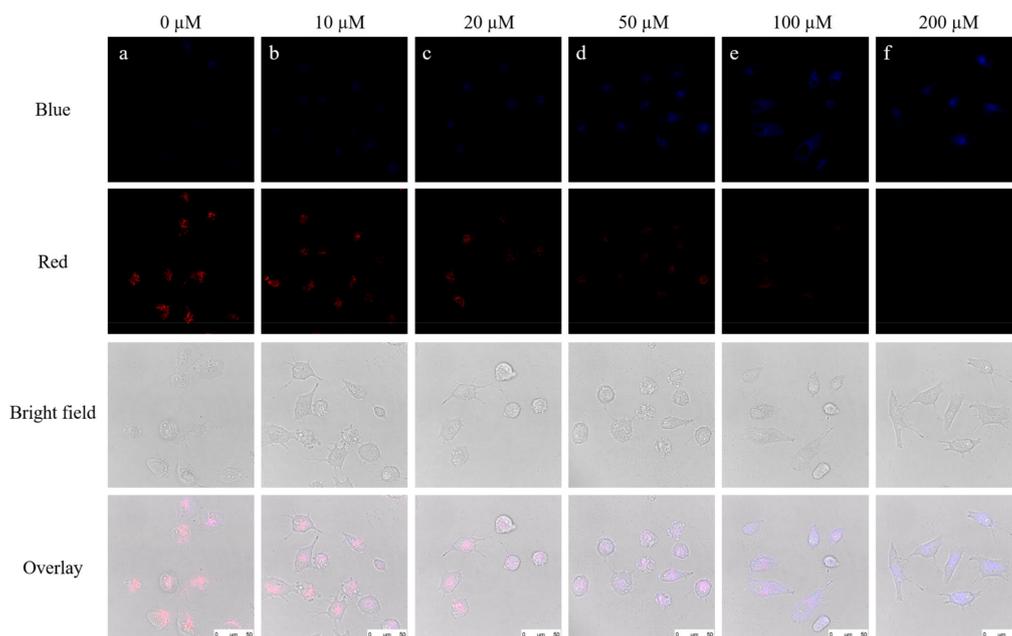
Figure 6. Imaging of SO_3^{2-} in HepG2 cells by the probe. The cells were stained with (**a**) 10 μM probe **EB** for 2 h; (**b**) 10 μM SO_3^{2-} for 2 h, 10 μM probe **EB** for 2 h; (**c**) 20 μM SO_3^{2-} for 2 h, 10 μM probe **EB** for 2 h; (**d**) 50 μM SO_3^{2-} for 2 h, 10 μM probe **EB** for 2 h; (**e**) 100 μM SO_3^{2-} for 2 h, 10 μM probe **EB** for 2 h; (**f**) 200 μM SO_3^{2-} for 2 h, 10 μM probe **EB** for 2 h; Blue channel: λ_{ex} = 405 nm; λ_{em} = 450–490 nm; Red channel: λ_{ex} = 488 nm; λ_{em} = 550–590 nm.

3. Materials and Methods

3.1. Materials and Instrumentation

The chemistry reagents (chemical grade) used in experiments was obtained from Sino Pharm Chemical Reagent Co. Ltd. (Shanghai, China). The real samples river water and tap water were obtained from the Shanghai University of Traditional Chinese Medicine, and sugar was purchased from a local supermarket (Shanghai, China). The chrysanthemum was purchased from Shanghai Kangqiao Chinese Medicine, grown in HangZhou, China. The analytical thin-layer chromatography (TLC) with pre-coated silica gel GF254 plates (Sino Pharm Chemical Reagent Co. Ltd., Shanghai, China) was used to detect any spots at 254 nm under UV light. ^{1}H-NMR and ^{13}C-NMR spectra were measured at 25 °C and referenced to tetramethyl silane (TMS) by a BRUKER AVANCE III spectrometer (Bruker, German). Electron ionization mass spectra (ESI-MS) was recorded on an Agilent 6460 triple quad LC-MS mass spectrometer (Agilent, Santa Clara, CA, USA). UV-Vis spectra and fluorescence spectra were recorded by Agilent 8454 UV-Vis spectrometer (Agilent) and Agilent G9800A fluorescence spectrophotometer (Agilent) respectively. Leica TCS-SP8 multiphoton illustrated the fluorescence images with the confocal microscope having a 63 × oil-immersion objective lens (Leica, Wetzlar, German).

3.2. Preparation of Probe *EB*

In a two-neck round-bottom flask, compound **1**, 3-ethyl-1,1,2-trimethyl-1*H*-benzo[e]indol-3-ium iodide (200.0 mg, 0.55 mM) and anhydrous ethanol (20 mL) were added. Subsequently, compound **2**, 4-hydroxybenzaldehyde (66.9 mg, 0.55 mM) was added to the mixture. This mixture reacted at 80 °C for 12 h. Then, the solution was disposed in a rotary vacuum desiccator and the solid was extracted with CH_2Cl_2/H_2O. The organic layer was collected and dried via anhydrous Na_2SO_4. The crude

product was purified with the CH_2Cl_2/MeOH eluent using the silica-gel column, see Supplementary Materials. Yield: 220 mg (87%). ESI/MS *m/z*: 342.34 [M]$^+$; ^{1}H-NMR (600 MHz, DMSO-d_6) δ 10.86 (s), 8.52 (d, *J.* = 16.1 Hz), 8.42 (d, *J.* = 8.5 Hz), 8.30 (d, *J.* = 8.9 Hz), 8.25 – 8.16 (m), 8.12 (d, *J.* = 8.9 Hz), 7.81 (t, *J.* = 7.6 Hz), 7.72 (t, *J.* = 7.5 Hz), 7.53 (d, *J.* = 16.2 Hz), 7.00 (d, *J.* = 8.7 Hz), 4.90 – 4.72 (m), 2.03 (s), 1.50 (t, *J.* = 7.2 Hz). ^{13}C-NMR (150 MHz, DMSO-d_6) δ 196.44, 138.68, 137.51, 133.51, 131.20, 130.21, 128.89, 127.76, 127.73, 123.90, 113.66, 55.94, 43.80, 21.95, 14.10.

3.3. Preparation of Solutions and Spectra Measurements

The probe was dissolved in ethyl alcohol to prepare the 1 mM stock solution. The anion and amino acid solution such as CO_3^{2-}, HCO_3^-, Ac$^-$, PO_4^{3-}, HPO_4^{2-}, $H_2PO_4^-$, Cl$^-$, Br$^-$, I$^-$, NO_2^-, S^{2-}, SO_4^{2-}, Hcy, Cys, GSH and SO_3^{2-} were all prepared by corresponding saline solution in purified water (10 mM). A small amount of stock probe **EB** (10 μM) and SO_3^{2-} (500 μM) were transferred to a 5 mL volumetric flask, diluted with PBS (pH = 7.4) to volume as the test solution at room temperature, which was prepared to measure fluorescent spectra and UV-Vis absorption. The test solution should be shaken well and detected after 3 min. The same volume of SO_3^{2-} solution could be replaced by various anion solutions mentioned above to detect interference using the same condition of spectra.

3.4. Measurements of Sulfite in Real Samples

Four kinds of samples: tap water, river water, sugar and chrysanthemum were prepared to detect sulfite respectively. Sugar and River water were diluted with PBS to a concentration of around 25 % (pH = 7.4) as the diluent solution. And the chrysanthemum sample was extracted with PBS solution (pH = 7.4) as the test solution (0.5 g/100 mL). Then transferred stock probe solution (10 μM) to a 5 mL volumetric flask, diluted with the diluent solution to volume. Incubated for 5 min at room temperature before detection. By the way, the recovery test also needed to add accurate SO_3^{2-} (25, 50 or 100 μM) in water samples. Then, the emission intensities at 473 nm and 570 nm were detailed and the analysis results were also compared with that achieved by the titration method.

3.5. Methods for Fluorescent Quantum Yield

The fluorescent quantum yields of probe **EB** and probe **EB** after reaction with SO_3^{2-} were detected using Rhodamine B (Φs = 0.89 in ethanol) as a standard. The Fluorescent quantum yields were determined based on the Equation:

$$\Phi_a = \Phi_{st} \times (F_a/F_{st}) \times (A_{st}/A_a) \times (\eta_a/\eta_{st})^2$$

where Φ presents the fluorescent quantum yield, A presents the absorbance at the excitation wavelength of the probe and standard respectively, F presents the integrated fluorescence intensity of the sample and standard at their excitation wavelength, η presents the refractive index of solvent.

3.6. Limit of Detection

The detection limit (LOD) was calculated based on the fluorescence titration of the probe (10 μM) in the presence of SO_3^{2-}. The fluorescence intensity ratio of the probe was measured and the standard deviation of the blank measurement was achieved. The limit of detection was calculated according to the following formula: LOD = 3σ/k

LOD: detection limit; σ: the standard deviation of the fluorescence intensity ratio (I_{473}/I_{570}) of the probe scanning for 10 times; k: the slope of the line graph of fluorescence intensity ratio (I_{473}/I_{570}) and reactant concentration.

3.7. Cell Culture and Fluorescence Imaging

HepG2 cells came from the Chinese Academy of Sciences. The cells were cultured in Dulbecco's modified Eagle's medium (DMEM) added with 1% Penicillin-Streptomycin Solution (100×), 10% fetal

bovine serum (FBS) at 37 °C under the atmosphere containing 5% CO_2. Then transferred cells to confocal dishes and waited for 24 h to keep adaption.

To inspect the sensitivity of the probe, cells were incubated in 10 μM probe for 2 h at 37 °C with culture medium (90% DMEM, 10% FBS). To detect exogenetic sulfite, cells were pretreated with different concentrations of SO_3^{2-} (0–200 μM) at 37 °C for 2 h and then incubated with the probe (10 μM) for 2 h. Before the detection achieved by the apparatus of Fluorescence Microscope and a 63× oil-immersion objective lens (Leica), cells needed to be washed by PBS for three times. The cells were stimulated by the intensity of wavelengths at 405 nm, 488 nm, and collected emission on 450–490 nm, 550–590 nm.

4. Conclusions

On the basis of the Michael addition reaction, we developed a new ratiometric fluorescent probe **EB** for SO_3^{2-}/HSO_3^- detection under physiological pH, which exhibited a colorimetric and ratiometric response to SO_3^{2-}/HSO_3^-. It could demonstrate a quick response, high sensitivity and selectivity to SO_3^{2-}/HSO_3^- in aqueous solution and real samples. The sensing mechanism of the interaction between the probe and SO_3^{2-}/HSO_3^- was verified using ESI-MS. Moreover, it exhibited the excellent application of detecting SO_2 derivatives in living cells with low cytotoxicity. All the results suggested this safe and harmless probe could be used conveniently.

Supplementary Materials: The following are available online. Figure S1. ^{1}H-NMR spectrum of the probe in DMSO-d_6; Figure S2. ^{13}C-NMR spectrum of compound the probe in DMSO-d_6; Figure S3. Mass spectrum of compound the probe. Table S1: Comparison of the probe for the detection of SO_3^{2-}/HSO_3^-.

Author Contributions: Conceived and designed the experiments: Y.D. and J.-S.L. Performed research and analyzed the data: X.-Y.J., Y.-H.Q., T.W., Y.-F.Q., J.-Y.G., A.A., K.-X.S., W.-Y.K. and B.-Y.H.; Wrote the paper: X.-Y.J., T.Z. and Y.-H.Q. All authors read and approved the final manuscript.

Conflicts of Interest: The authors declare no conflict of interest.

References

1. Meng, Z.; Qin, G.; Zhang, B.; Bai, J. DNA damaging effects of sulfur dioxide derivatives in cells from various organs of mice. *Mutagenesis* **2004**, *19*, 465–468. [CrossRef]
2. Shi, X. Generation of SO_3^- and OH radicals in SO_3^{2-} reactions with inorganic environmental pollutants and its implications to SO_3^{2-} toxicity. *J. Inorg. Biochem.* **1994**, *56*, 155–165. [CrossRef]
3. Yin, C.X.; Li, X.Q.; Yue, Y.K.; Chao, J.B.; Zhang, Y.B.; Huo, F.J. A new fluorescent material and its application in sulfite and bisulfite bioimaging. *Sens. Actuat. B-Chem.* **2017**, *246*, 615–622. [CrossRef]
4. Meng, Z.; Yang, Z.; Li, J.; Zhang, Q. The vasorelaxant effect and its mechanisms of sodium bisulfite as a sulfur dioxide donor. *Chemosphere* **2012**, *89*, 579–584. [CrossRef]
5. Stipanuk, M.H.; Ueki, I. Dealing with methionine/homocysteine sulfur: Cysteine metabolism to taurine and inorganic sulfur. *J. Inherit. Metab. Dis.* **2011**, *34*, 17–32. [CrossRef] [PubMed]
6. Huang, H.; Liu, W.; Liu, X.J.; Kuang, Y.Q.; Jiang, J.H. A novel mitochondria-targeted near-infrared fluorescence probe for ultrafast and ratiometric detection of SO_2 derivatives in live cells. *Talanta* **2017**, *168*, 203–209. [CrossRef]
7. Iwasawa, S.; Kikuchi, Y.; Nishiwaki, Y.; Nakano, M.; Michikawa, T.; Tsuboi, T.; Tanaka, S.; Uemura, T.; Ishigami, A.; Nakashima, H.; et al. Effects of SO_2 on respiratory system of adult Miyakejima resident 2 years after returning to the island. *J. Occup. Health* **2009**, *51*, 38–47. [CrossRef]

8.   Chen, T.M.; Gokhale, J.; Shofer, S.; Kuschner, W.G. Outdoor air pollution: Nitrogen dioxide, sulfur dioxide, and carbon monoxide health effects. *Am. J. Med. Sci.* **2007**, *333*, 249–256. [CrossRef]

9.   Schneider, M.; Turke, A.; Fischer, W.J.; Kilmartin, P.A. Determination of the wine preservative sulphur dioxide with cyclic voltammetry using inkjet printed electrodes. *Food Chem.* **2014**, *159*, 428–432. [CrossRef]

10. Grings, M.; Moura, A.P.; Parmeggiani, B.; Pletsch, J.T.; Cardoso, G.M.F.; August, P.M.; Matte, C.; Wyse, A.T.S.; Wajner, M.; Leipnitz, G. Bezafibrate prevents mitochondrial dysfunction, antioxidant system disturbance, glial reactivity and neuronal damage induced by sulfite administration in striatum of rats: Implications for a possible therapeutic strategy for sulfite oxidase deficiency. *Biochim. Biophys. Acta. Mol. Basis. Dis.* **2017**, *1863*, 2135–2148. [CrossRef]

11. Chen, W.; Fang, Q.; Yang, D.; Zhang, H.; Song, X.; Foley, J. Selective, Highly Sensitive Fluorescent Probe for the Detection of Sulfur Dioxide Derivatives in Aqueous and Biological Environments. *Anal. Chem.* **2014**, *87*, 609–616. [CrossRef]

12. Xiang, K.; Chang, S.; Feng, J.; Li, C.; Ming, W.; Liu, Z.; Liu, Y.; Tian, B.; Zhang, J. A colorimetric and ratiometric fluorescence probe for rapid detection of SO_2 derivatives bisulfite and sulfite. *Dye. Pigment.* **2016**, *134*, 190–197. [CrossRef]

13. Rajantie, H.; Williams, D.E. Electrochemical titrations of thiosulfate, sulfite, dichromate and permanganate using dual microband electrodes. *Analyst* **2001**, *126*, 86–90. [CrossRef] [PubMed]

14. Türke, A.; Fischer, W.J.; Beaumont, N.; Kilmartin, P.A. Electrochemistry of sulfur dioxide, polyphenols and ascorbic acid at poly(3,4-ethylenedioxythiophene) modified electrodes. *Electrochim. Acta.* **2012**, *60*, 184–192. [CrossRef]

15. O'Brien, J.A.; Hinkley, J.T.; Donne, S.W.; Lindquist, S.E. The electrochemical oxidation of aqueous sulfur dioxide: A critical review of work with respect to the hybrid sulfur cycle. *Electrochim. Acta.* **2010**, *55*, 573–591. [CrossRef]

16. Sullivan, J.; Douek, M. Analysis of hydroxide, inorganic sulphur species and organic anions in kraft pulping liquors by capillary electrophoresis. *J. Chromatogr. A* **2004**, *1039*, 215–225. [CrossRef] [PubMed]

17. Hirata, K.; Ito, K.; Hirokado, M.; Uematsu, Y.; Suzuki, K.; Suzuki, S.; Saito, K. Determination of sulfur dioxide content of grape skin extract and elderberry color by capillary electrophoresis. *Shokuhin. Eiseigaku. Zasshi* **2000**, *41*, 144–148. [CrossRef]

18. Zhou, H.; Tang, J.B.; Zhang, J.; Chen, B.C.; Kan, J.F.; Zhang, W.F.; Zhou, J.; Ma, H.M. A red lysosome-targeted fluorescent probe for carboxylesterase detection and bioimaging. *J. Mater. Chem. B* **2019**, *7*, 2989–2996. [CrossRef]

19. Sun, Y.; Zhao, D.; Fan, S.; Duan, L.; Li, R. Ratiometric fluorescent probe for rapid detection of bisulfite through 1,4-addition reaction in aqueous solution. *J. Agric. Food Chem.* **2014**, *320*, 62–3405. [CrossRef]

20. Tan, L.; Lin, W.; Zhu, S.; Yuan, L.; Zheng, K. A coumarin-quinolinium-based fluorescent probe for ratiometric sensing of sulfite in living cells. *Org. Biomol. Chem.* **2014**, *12*, 4637–4643. [CrossRef]

21. Li, D.P.; Wang, Z.Y.; Cui, J.; Wang, X.; Miao, J.Y.; Zhao, B.X. A new fluorescent probe for colorimetric and ratiometric detection of sulfur dioxide derivatives in liver cancer cells. *Sci. Rep.-UK* **2017**, *7*, 45294–45301.

22. Niu, T.T.; Yu, T.; Yin, G.X.; Chen, H.M.; Yin, P.; Li, H.T. A novel colorimetric and ratiometric fluorescent probe for sensing SO2 derivatives and their bio-imaging in living cells. *Analyst* **2019**, *144*, 1546–1554. [CrossRef] [PubMed]

23. Wang, G.; Qi, H.; Yang, X.F. A ratiometric fluorescent probe for bisulphite anion, employing intramolecular charge transfer. *Luminescence* **2013**, *28*, 97–101. [CrossRef] [PubMed]

24. Li, M.; Feng, W.; Zhai, Q.; Feng, G. Selenocysteine detection and bioimaging in living cells by a colorimetric and near-infrared fluorescent turn-on probe with a large stokes shift. *Biosens. Bioelectron.* **2017**, *87*, 894–900. [CrossRef] [PubMed]

25. Yu, T.; Yin, G.; Niu, T.; Yin, P.; Li, H.; Zhang, Y.; Chen, H.; Zeng, Y.; Yao, S. A novel colorimetric and fluorescent probe for simultaneous detection of SO32–/HSO3– and HSO4– by different emission channels and its bioimaging in living cells. *Talanta* **2018**, *176*, 1–7. [CrossRef] [PubMed]

26. Sun, Q.; Zhang, W.; Qian, J. A ratiometric fluorescence probe for selective detection of sulfite and its application in realistic samples. *Talanta* **2017**, *162*, 107–113. [CrossRef] [PubMed]

27. Zhang, H.; Huang, Z.; Feng, G. Colorimetric and ratiometric fluorescent detection of bisulfite by a new HBT-hemicyanine hybrid. *Anal. Chim. Acta.* **2016**, *920*, 72–79. [CrossRef]

28. Xu, W.; Teoh, C.L.; Peng, J.; Su, D.; Yuan, L.; Chang, Y.T. A mitochondria-targeted ratiometric fluorescent probe to monitor endogenously generated sulfur dioxide derivatives in living cells. *Biomaterials* **2015**, *56*, 1–9. [CrossRef]

29. Lan, J.S.; Zeng, R.F.; Ding, Y.; Zhang, Y.; Zhang, T.; Wu, T. A simple pyrene–hemicyanine fluorescent probe for colorimetric and ratiometric detection of SO$_2$ derivatives in the mitochondria of living cells and zebrafish in vivo. *Sens. Actuators B Chem.* **2018**, *268*, 328–337. [CrossRef]

30. Li, C.; Plamont, M.A.; Aujard, I.; Le Saux, T.; Jullien, L.; Gautier, A. Design and characterization of red fluorogenic push-pull chromophores holding great potential for bioimaging and biosensing. *Org. Biomol. Chem.* **2016**, *14*, 9253–9261. [CrossRef]

31. Xu, J.; Zhang, Y.; Yu, H.; Gao, X.; Shao, S. Mitochondria-Targeted Fluorescent Probe for Imaging Hydrogen Peroxide in Living Cells. *Anal. Chem.* **2016**, *88*, 1455–1461. [CrossRef] [PubMed]

32. Nie, J.; Liu, Y.; Niu, J.; Ni, Z.; Lin, W. A new pyrene-based fluorescent probe with large Stokes shift for detecting hydrogen peroxide in aqueous solution and living cells. *J. Photochem. Photobiol. A Chem.* **2017**, *348*, 1–7. [CrossRef]

33. Kumar, A.; Pandith, A.; Kim, H.-S. Pyrene-appended imidazolium probe for 2,4,6-trinitrophenol in water. *Sens. Actuators B Chem.* **2016**, *231*, 293–301. [CrossRef]

34. Zhu, L.; Xu, J.; Sun, Z.; Fu, B.; Qin, C.; Zeng, L.; Hu, X. A twisted intramolecular charge transfer probe for rapid and specific detection of trace biological SO$_2$ derivatives and bio-imaging applications. *Chem. Commun.* **2015**, *51*, 1154–1156. [CrossRef]

Sample Availability: Not available.